weight could be a natural corollary of the theoretical expectation[17] that polymer interfacial tension, i.e. surface free energy, should increase with increasing chain length (owing to entropic constraints at the surface). Data do not appear to be available for $\sigma_{\mathrm{W-P}}$, but this has long been known to occur for $\sigma_{\mathrm{P-A}}$.[18]

In summary, a phase diagram not previously reported for amorphous polymers at submonolayer coverage has been described. A spreading transition was observed with increasing molecular weight.

Acknowledgment. We thank M. Wortis for comments. This work was supported by Grant DMR-86-12860 from the National Science Foundation. Acknowledgement is also made to the Research Corp. and to the donors of the Petroleum Research Fund, administered by the American Chemical Society, for partial support of this research. S.J.C. thanks the Science and Engineering Council (U.K.) for a fellowship.

References and Notes

(1) Gaines, G. L., Jr. *Insoluble Monolayers at Liquid-Gas Interfaces*: Interscience: New York, 1966.
(2) Granick, S. *Macromolecules* **1985**, *18*, 1597.
(3) Crisp, D. J. In *Surface Phenomena in Chemistry and Biology*; Danielli, J. F., Pankhurst, K. G. A., Riddiford, A. C., Eds.; Pergamon: New York, 1958.
(4) Vilanove, R.; Rondelez, R. *Phys. Rev. Lett* **1980**, *45*, 1502.
(5) Takahashi, A.; Yoshida, A.; Kawaguchi, M. *Macromolecules* **1983**, *15*, 1196.
(6) Pandit, R.; Schick, M.; Wortis, M. *Phys. Rev. B; Condens. Matter* **1982**, *26*, 5112.
(7) de Gennes, P.-G. *Rev. Mod. Phys.* **1985**, *57*, 827.
(8) Clarson, S. J.; Semlyen, J. A. *Polymer* **1986**, *27*, 1633.
(9) Clarson, S. J.; Dodgson, K.; Semlyen, J. A. *Polymer* **1987**, *28*, 189.
(10) Clarson, S. J.; Mark, J. G.; Clarson, S. J.; Dodgson, K.; Semlyen, J. A. *Polymer*, in press.
(11) Ausserê, D.; Picard, A. M.; Léger, L. *Phys. Rev. Lett.* **1987**, *57*, 2671.
(12) Kuzmenka, D. J.; Granick, S. *Macromolecules* **1988**, *21*, 779.
(13) Ter-Minassian-Saraga, L.; Prigogine, I. *Mem. Serv. Chim. Etat (Paris)* **1953**, *38*, 109.
(14) Wortis, M., private communication.
(15) Cohen-Stuart, M. A., private communication.
(16) Derjaguin, B. V.; Churaev, N. V.; Müller, V. M. *Surface Forces*; Consultants Bureau: New York, 1987.
(17) Theodorou, D. *Macromolecules* **1988**, *21*, 1400.
(18) Wu, S. *Polymer Interface and Adhesion*; Marcel Dekker: New York, 1982; Chapter 3.

Matrix Representation of the Dynamical Structure Factor of a Solution of Rodlike Polymers in the Isotropic Phase

Tadakazu Maeda

Mitsubishi Kasei Institute of Life Sciences, 11 Minami-ooya, Machida-shi, Tokyo 194, Japan. *Received July 11, 1988; Revised Manuscript Received October 10, 1988*

ABSTRACT: The dynamical structure factor of a solution of rodlike polymers, recently derived by Doi, Shimada, and Okano (*J. Chem. Phys.* **1988**, *88*, 4070), was rewritten in matrix form, the evaluation of which is quite easy and straightforward. With this formulation, it is possible to compute the dynamic light scattering spectrum of rigid rod suspensions in the entire region of $\mathbf{k}$, t, and ν, where $\mathbf{k}$ is the scattering vector, t the delay time, and ν the number concentration of the rods. Results of numerical computation show that the excluded-volume interaction affects only the spatially long and temporarily slow modes of fluctuation in the solution and suggest that it is necessary to generalize the osmotic virial coefficient A_2 as a function of kL, where L is the rod length. The present analysis raises the possibility of studying the concentration dependence of $D_\parallel$, $D_\perp$, and D_r individually, where $D_\parallel$ and $D_\perp$ are self-diffusion coefficients for the lengthways and sideways translation of a rod, respectively, and D_r is the rotational one.

1. Introduction

When we theoretically construct the dynamic light scattering (DLS) spectrum of rod suspensions at finite concentration, we have to take into account the translation-rotation coupling of rod diffusion and various types of rod-rod interactions: In general, the translational and rotational diffusive motions of a rod in solution are coupled with each other, because the friction constant parallel to the rod axis is smaller than that perpendicular to the axis. When the rod concentration increases, we can no longer neglect such types of rod-rod interactions as the excluded-volume interaction (the steric repulsion and van der Waals attraction between polymers), the entanglement effect (the topological constraint that filaments cannot pass through each other), and the hydrodynamic interaction.

Doi, Shimada, and Okano[1] (DSO) recently studied the dynamics of rodlike polymers in solution under the influence of other polymers, taking all the above four factors into account: They started from a kinetic equation for the average number density $f(\mathbf{r}, \mathbf{u}, t)$ of rods, where $\mathbf{r}$ is the position vector of the center of a rod and $\mathbf{u}$ the orientation unit vector of the long axis of the rod. The equation they adopted is the one that expresses the coupled diffusion of the translation and rotation of a rod:

$$\frac{\partial f}{\partial t} = \frac{\partial}{\partial \mathbf{r}}[D_{\parallel,0}\mathbf{u}\mathbf{u} + D_{\perp,0}(\mathbf{I} - \mathbf{u}\mathbf{u})]\left[\frac{\partial f}{\partial \mathbf{r}} + \frac{f}{k_\mathrm{B}T}\frac{\partial h}{\partial \mathbf{r}}\right] + D_{\mathrm{r},0}\mathcal{R}\left[\mathcal{R}f + \frac{f}{k_\mathrm{B}T}\mathcal{R}h\right] \quad (1)$$

where $D_{\parallel,0}$ and $D_{\perp,0}$ are the lengthways and sideways translational diffusion coefficients, respectively, h is the potential of an external field, $D_{\mathrm{r},0}$ is the rotational diffusion coefficient, and $\mathcal{R}$ the rotational operator. The subscript 0 of $D_{\perp,0}$, $D_{\perp,0}$, and $D_{\mathrm{r},0}$ denotes zero polymer concentration, and since eq 1 includes no interactions between rods, it holds only in the dilute regime.

Next, they took into account the excluded-volume effect, using the mean-field approximation. Let $W(\mathbf{r} - \mathbf{r}', \mathbf{u}, \mathbf{u}')$ be the interaction potential between two polymers in the configurations $(\mathbf{r}, \mathbf{u})$ and $(\mathbf{r}', \mathbf{u}')$. In the mean-field approximation, the molecular field for a polymer in the configuration $(\mathbf{r}, \mathbf{u})$ is written as

$$\bar{W}(\mathbf{r}, \mathbf{u}, t) = \int \mathrm{d}\mathbf{r}' \int \mathrm{d}\mathbf{u}'\, W(\mathbf{r} - \mathbf{r}', \mathbf{u}, \mathbf{u}') f(\mathbf{r}', \mathbf{u}', t) \quad (2)$$

Therefore the kinetic equation for $f(\mathbf{r}, \mathbf{u}, t)$ at finite polymer concentration becomes

$$\frac{\partial f}{\partial t} = \frac{\partial}{\partial \mathbf{r}}[D_{\parallel}\mathbf{uu} + D_{\perp}(\mathbf{I} - \mathbf{uu})]\left[\frac{\partial f}{\partial \mathbf{r}} + f\frac{\partial}{\partial \mathbf{r}}(h + \bar{W})\right] + D_{\mathrm{r}}\mathcal{R}[\mathcal{R}f + f\mathcal{R}(h + \bar{W})] \quad (3)$$

where $k_{\mathrm{B}}T$ has been set to unity. Note that diffusion coefficients $D_{\parallel}$, $D_{\perp}$, and D_{r} in this equation are all self-diffusivities at finite polymer concentrations. DSO regarded these coefficients as adjustable parameters that depended on the polymer concentration, and thus they took into consideration the last two factors, the entanglement and hydrodynamic interactions.

Using the fluctuation–dissipation theorem, DSO derived from eq 3 an expression for the dynamical structure factor $g(\mathbf{k}, t)$ as

$$g(\mathbf{k}, t) = \frac{L}{4\pi}\int_t^{\infty}\mathrm{d}t' \int \mathrm{d}\mathbf{u}\ s_{\mathbf{k}}(\mathbf{u}) \exp[-t'\Omega_{\mathbf{k}}]\Theta_{\mathbf{k}}s_{\mathbf{k}}(\mathbf{u}) \quad (4)$$

where $\mathbf{k}$ is the scattering vector, $s_{\mathbf{k}}(\mathbf{u})$ the $\mathbf{k}$-component of the normalized electric field of the light scattered from a rod with orientation $\mathbf{u}$, $\Theta_{\mathbf{k}}$ the translational–rotational diffusion operator for a rod, and $\Omega_{\mathbf{k}} \equiv \Theta_{\mathbf{k}}\Phi_{\mathbf{k}}$. Operator $\Phi_{\mathbf{k}}$ expresses the rod–rod interaction. The function $s_{\mathbf{k}}(\mathbf{u})$ and operators $\Theta_{\mathbf{k}}$ and $\Phi_{\mathbf{k}}$ are defined by the following equations

$$s_{\mathbf{k}}(\mathbf{u}) = \frac{1}{L}\int_{-L/2}^{L/2}\exp(i\mathbf{k}\cdot\mathbf{u}s)\ \mathrm{d}s \quad (5)$$

$$\Theta_{\mathbf{k}}s_{\mathbf{k}}(\mathbf{u}) = [D_{\parallel}(\mathbf{k}\cdot\mathbf{u})^2 + D_{\perp}\{\mathbf{k}^2 - (\mathbf{k}\cdot\mathbf{u})^2\} - D_{\mathrm{r}}\mathcal{R}^2]s_{\mathbf{k}}(\mathbf{u}) \quad (6)$$

$$\Phi_{\mathbf{k}}s_{\mathbf{k}}(\mathbf{u}) = \int \mathrm{d}\mathbf{u}' \left[\delta(\mathbf{u} - \mathbf{u}') + \frac{\nu}{4\pi}W_{\mathbf{k}}(\mathbf{u}, \mathbf{u}')\right]s_{\mathbf{k}}(\mathbf{u}') \quad (7)$$

where L is the rod length, ν the number concentration of the rods, and $W_{\mathbf{k}}(\mathbf{u}, \mathbf{u}')$ the Fourier transform of $W(\mathbf{r} - \mathbf{r}', \mathbf{u}, \mathbf{u}')$. Assuming the rigid-body interaction potential for $W(\mathbf{r} - \mathbf{r}', \mathbf{u}, \mathbf{u}')$, we have

$$W_{\mathbf{k}}(\mathbf{u}, \mathbf{u}') = 2bL^2|\mathbf{u} \times \mathbf{u}'|s_{\mathbf{k}}(\mathbf{u})s_{\mathbf{k}}(\mathbf{u}') \quad (8)$$

where b is the rod diameter.

Unfortunately, it is difficult to evaluate eq 4, and DSO gave exact expressions only for two limiting cases, i.e., $\mathbf{k} \to 0$ and $t \to 0$. The DSO theory in these two cases qualitatively agreed with experiments, which encouraged us to rewrite their expression in a more tractable form. In order to compare the DSO theory with experiments, we do need an expression for $g(\mathbf{k}, t)$ which can be evaluated straightforwardly in the entire region of $\mathbf{k}$, t, and ν.

The aim of this paper is to give an expression for $g(\mathbf{k}, t)$ that satisfies such a requirement. The formulation given in this paper is nothing but a rewriting of the DSO theory, but it opens an easy path to computing the DLS spectrum of rod suspensions in the less dilute regime and will thus have practical importance. We also give expressions for the initial decay rate $\Gamma_{\mathbf{k}}$ and static structure factor, followed by results of numerical computation. Lastly, we discuss implications of the DSO theory through concentration and angular dependence of $\Gamma_{\mathbf{k}}/k^2$ and compare the theory with a number of experimental observations. It will also be shown that the formulation given in this paper is an extension of the one previously derived for dilute suspensions of rigid rods.[2]

2. Matrix Representation of $g(\mathbf{k}, t)$

Since operators $\Theta_{\mathbf{k}}$ and $\Phi_{\mathbf{k}}$ transform the function $s_{\mathbf{k}}(\mathbf{u})$ on the unit sphere, it seems at first sight that we have to use spherical tensors to express these operators. However, as will be shown later, we only need spherical harmonics $Y_{lm}(\mathbf{u})$ with $m = 0$ in the case of polarized light scattering, and it is possible to express the dynamical structure factor $g(\mathbf{k}, t)$ by using matrices and vectors.

2.1. Vector Representation of $s_{\mathbf{k}}(\mathbf{u})$. We take the scattering vector $\mathbf{k}$ as the polar axis and the angle between $\mathbf{k}$ and $\mathbf{u}$ as the polar angle θ. With this polar coordinate system, the function $s_{\mathbf{k}}(\mathbf{u})$ does not include the azimuthal angle ϕ, and we can expand $s_{\mathbf{k}}(\mathbf{u})$ with Legendre polynomials $P_l(\cos\theta)$ or spherical harmonics $Y_{lm}(\mathbf{u})$ with $m = 0$. Using the familiar Rayleigh expansion of a plane wave

$$\exp(i\mathbf{k}\cdot\mathbf{r}) = \sum_{l=0}^{\infty} i^l(2l + 1)j_l(kr)P_l(\cos\theta)$$

and the relation between $P_l(\cos\theta)$ and $Y_{lm}(\mathbf{u})$,

$$P_l(\cos\theta) = \left[\frac{4\pi}{2l + 1}\right]^{1/2} Y_{l,0}(\mathbf{u})$$

we have a column vector $\mathbf{s}$, the lth element of which is

$$\begin{aligned} s_l &= \frac{1}{(4\pi)^{1/2}}\int \mathrm{d}\mathbf{u}\ s_{\mathbf{k}}(\mathbf{u})Y_{l,0}(\mathbf{u}) \\ &= 0 \qquad \text{for odd } l \\ &= (-1)^{l/2}(2l + 1)^{1/2}b_l(K) \qquad \text{for even } l \end{aligned} \quad (9)$$

where

$$b_l(K) = \frac{1}{K}\int_0^K j_l(x)\ \mathrm{d}x \quad (10)$$

$$K = kL/2 \quad (11)$$

and $j^l(x)$ is the lth-order spherical Bessel function.

2.2. Matrix Representation of $\Theta_{\mathbf{k}}$. Since $\cos^2\theta = (1/3)\{2(4\pi/5)^{1/2}Y_{2,0}(\mathbf{u}) + 1\}$, we have

$$\Theta_{\mathbf{k}} = D_{\mathrm{G}}k^2 + \frac{2}{3}\left[\frac{4\pi}{5}\right]^{1/2}(D_{\parallel} - D_{\perp})k^2Y_{2,0}(\mathbf{u}) - D_{\mathrm{r}}\mathcal{R}^2 \quad (12)$$

where D_{G}, defined by $D_{\mathrm{G}} \equiv (2D_{\perp} + D_{\parallel})/3$, is the self-diffusivity of the center of gravity of a rod. Let $\boldsymbol{\Theta}$ be a matrix that corresponds to operator $\Theta_{\mathbf{k}}$. We compute the ll'-element of matrix $\boldsymbol{\Theta}$ as

$$\Theta_{ll'} = \int \mathrm{d}\mathbf{u}\ Y^*_{l,0}(\mathbf{u})\Theta_{\mathbf{k}}Y_{l',0}(\mathbf{u}) = \{D_{\mathrm{G}}k^2 + D_{\mathrm{r}}l(l + 1)\}\delta_{ll'} + \frac{2}{3}\left[\frac{4\pi}{5}\right]^{1/2}(D_{\parallel} - D_{\perp})k^2\int \mathrm{d}\mathbf{u}\ Y^*_{l,0}(\mathbf{u})Y_{2,0}(\mathbf{u})Y_{l',0}(\mathbf{u})$$

where we used the orthonormality of spherical harmonics and the fact that $Y_{lm}(\mathbf{u})$ is the eigenfunction of operator $\mathcal{R}^2$.

We use a formula for the integral of three spherical harmonics[3]

$$\int \mathrm{d}\mathbf{u}\ Y^*_{l_3m_3}Y_{l_2m_2}Y_{l_1m_1} = \left[\frac{(2l_1 + 1)(2l_2 + 1)}{4\pi(2l_3 + 1)}\right]^{1/2} C(l_1l_2l_3;m_1m_2m_3)C(l_1l_2l_3;000) \quad (13)$$

where $C(l_1l_2l_3;m_1m_2m_3)$ is the Clebsch–Gordan or C coefficient. From the properties of the C coefficient that

$$C(l_1l_2l_3;000) = 0 \qquad \text{unless} \quad l_1 + l_2 + l_3 \text{ is even}$$

it is evident that $\Theta_{ll'} = 0$ unless the subscripts l and l' have the same parity. From the triangular condition for the coupling of l_1, l_2, and l_3 (the C coefficient vanishes unless $l_3 = l_1 + l_2, l_1 + l_2 - 1, ..., |l_1 - l_2|$), it is also clear that $\Theta_{ll'} = 0$ unless $l = l'$ or $l' \pm 2$; i.e., $\boldsymbol{\Theta}$ is a tridiagonal matrix. Racah's expression[3] for $C(l_1l_2l_3;000)$ is very useful when we derive an explicit form of $\Theta_{ll'}$.

$$C(l_1l_2l_3;000) = (-1)^{(l_1+l_2-l_3)/2}\left[\frac{2l_3+1}{l_1+l_2+l_3+1}\right]^{1/2}\times \frac{\tau(l_1+l_2+l_3)}{\tau(l_1+l_2-l_3)\tau(l_1-l_2+l_3)\tau(-l_1+l_2+l_3)} \tag{14}$$

where $l_1 + l_2 + l_3$ is an even integer and

$$\tau(x) = (x/2)!/(x!)^{1/2}$$

After some rearrangement, matrix Θ is expressed as

$$\Theta = D_\perp k^2\mathbf{E} + D_r(\mathbf{R} + \mu^2\mathbf{T}) \tag{15}$$

where $\mathbf{E}$ is an identity matrix, $\mathbf{R}$ a rotational eigenvalue matrix, $\mathbf{T}$ a symmetric tridiagonal matrix that expresses the anisotropic translation, and μ^2 the coupling constant between $\mathbf{R}$ and $\mathbf{T}$.

$$\mathbf{R}_{ll'} = l(l+1)\delta_{ll'} \tag{16}$$

$$\mathbf{T}_{l,l-2} = \mathbf{T}_{l-2,l} = \frac{l(l-1)}{(2l-1)[(2l-3)(2l+1)]^{1/2}} \tag{17}$$

$$\mathbf{T}_{ll} = \frac{2l^2+2l-1}{(2l-1)(2l+3)} \tag{18}$$

$$\mu^2 = (D_\parallel - D_\perp)k^2/D_r \tag{19}$$

Matrix elements $\mathbf{T}_{ll'}$ with $l \neq l', l' \pm 2$ are all zero.

2.3. Matrix Representation of $\Phi_\mathbf{k}$. Let $\mathbf{W}$ be a matrix that corresponds to the operator

$$\mathbf{W}s_\mathbf{k}(\mathbf{u}) = (1/4\pi^2bL^2)\int d\mathbf{u}'\ W_\mathbf{k}(\mathbf{u},\mathbf{u}')s_\mathbf{k}(\mathbf{u}')$$

To compute the ll' element of matrix $\mathbf{W}$, we use a formula[4] that expresses $|\mathbf{u}\times\mathbf{u}'|$ in terms of spherical harmonics

$$|\mathbf{u}\times\mathbf{u}'| = \frac{\pi}{2}\left[\frac{1}{2} - \sum_{\substack{p=2\\ \text{even}}}^{\infty}\frac{4\pi(p-1)}{p+2}\left\{\frac{(p-3)!!}{p!!}\right\}^2\sum_m Y^*_{pm}(\mathbf{u}')Y_{pm}(\mathbf{u})\right] \tag{20}$$

where $(2n)!! = 2n(2n-2)\cdots4\cdot2$, $(2n-1)!! = (2n-1)(2n-3)\cdots3\cdot1$, and $0!! = (-1)!! = 1$.

Using eq 20, we have

$$\mathbf{W}_{ll'} = \frac{1}{4\pi^2bL^2}\int d\mathbf{u}\ Y^*_{l,0}(\mathbf{u})\int d\mathbf{u}'\ W_\mathbf{k}(\mathbf{u},\mathbf{u}')Y_{l',0}(\mathbf{u}') = \frac{1}{8\pi}\int d\mathbf{u}\ Y^*_{l,0}(\mathbf{u})s_\mathbf{k}(\mathbf{u})\int d\mathbf{u}'\ s_\mathbf{k}(\mathbf{u}')Y_{l',0}(\mathbf{u}') - \sum_{\substack{p=2\\ \text{even}}}^{\infty}\frac{p-1}{p+2}\left[\frac{(p-3)!!}{p!!}\right]^2\sum_m\int d\mathbf{u}\ Y^*_{l,0}(\mathbf{u})s_\mathbf{k}(\mathbf{u})Y_{pm}(\mathbf{u})\times\int d\mathbf{u}'\ Y^*_{pm}(\mathbf{u}')s_\mathbf{k}(\mathbf{u}')Y_{l'0}(\mathbf{u}') \tag{21}$$

Since $s_\mathbf{k}(\mathbf{u}) = (4\pi)^{1/2}\sum_n s_nY_{n,0}(\mathbf{u})$, we have for the integrals in eq 21

$$\int d\mathbf{u}\ Y^*_{l,0}(\mathbf{u})s_\mathbf{k}(\mathbf{u})Y_{pm}(\mathbf{u}) = \left[\frac{2p+1}{2l+1}\right]^{1/2}\sum_{n:\text{even}}(-1)^{n/2}(2n+1)b_n(K)C(pnl;000)^2\delta_{m0}$$

$$\int d\mathbf{u}'\ Y^*_{pm}(\mathbf{u}')s_\mathbf{k}(\mathbf{u}')Y_{l'0}(\mathbf{u}') = \left[\frac{2l'+1}{2p+1}\right]^{1/2}\sum_{n:\text{even}}(-1)^{n/2}(2n+1)b_n(K)C(l'np;000)^2\delta_{m0}$$

where we used eq 13 and the properties of the C coefficient that

$$C(l_1l_2l_3;m_1m_2m_3) = 0 \qquad \text{unless} \quad m_3 = m_1 + m_2$$

We have now an explicit form of matrix $\mathbf{W}$ as

$$\mathbf{W} = \frac{1}{2}\mathbf{s}\mathbf{s}^\mathrm{T} - \mathbf{PQP} \tag{22}$$

where $\mathbf{s}^\mathrm{T}$ is the transposition of the column vector $\mathbf{s}$, $\mathbf{P}$ a symmetrical matrix, and $\mathbf{Q}$ a diagonal one:

$$\mathbf{P}_{lp} = \left[\frac{2p+1}{2l+1}\right]^{1/2}\sum_{n:\text{even}}(-1)^{n/2}(2n+1)b_n(K)C(pnl;000)^2 \tag{23}$$

$$\mathbf{Q}_{pp} = \frac{p-1}{p+2}\left[\frac{(p-3)!!}{p!!}\right]^2 \qquad \text{for} \quad p = 2, 4, \ldots \tag{24}$$

The index n of summation in eq 23 runs through even integers from $|p - l|$ to $p + l$. Matrix $\mathbf{P}$ is symmetrical because of the symmetry of the C coefficient

$$C(l_1l_2l_3;m_1m_2m_3) = (-1)^{l_2-m_2}\left[\frac{2l_3+1}{2l_1+1}\right]^{1/2}C(l_3l_2l_1;-m_3,m_2,-m_1)$$

Matrix elements $\mathbf{Q}_{pp}$ with $p = 0$ and odd p are all zero. Using eq 22, we easily have matrix Φ that corresponds to operator $\Phi_\mathbf{k}$ as

$$\Phi = \mathbf{E} + \pi\nu bL^2\mathbf{W} \tag{25}$$

Expressions for matrix $\mathbf{W}$ in the limit of $\mathbf{k} \to 0$ and $\mathbf{k} \to \infty$ are given in the Appendix.

2.4. Eigenvalue Problem and Matrix Representation of $g(\mathbf{k},t)$. Let Ω be a matrix that corresponds to operator $\Omega_\mathbf{k}$. Using eq 15 and 25, we simply have $\Omega = \Theta\Phi$. Let $\mathbf{U}$ and Λ be the eigenvector and eigenvalue matrices of Ω, respectively:

$$\Omega\mathbf{U} = \mathbf{U}\Lambda$$

Since $\exp[-\Omega t'] = \mathbf{U}\exp[-\Lambda t']\mathbf{U}^{-1}$ and since $\exp[-\Lambda t']$ is a diagonal matrix, we can easily carry out the integration in eq 4 with respect to t':

$$g(\mathbf{k},t) = L\int_t^\infty dt'\,\mathbf{s}^\mathrm{T}\mathbf{U}\exp[-\Lambda t']\mathbf{U}^{-1}\Theta\mathbf{s} = L\mathbf{s}^\mathrm{T}\mathbf{U}\exp[-\Lambda t]\Lambda^{-1}\mathbf{U}^{-1}\Theta\mathbf{s} = L\mathbf{s}^\mathrm{T}\mathbf{U}\exp[-\Lambda t]\mathbf{U}^{-1}\Phi^{-1}\mathbf{s} \tag{26}$$

The main result of this paper is eq 26, which gives the dynamical structure factor in the matrix representation.

2.5. Initial Decay Rate. We can easily derive from eq 26 an expression for the initial decay rate $\Gamma_\mathbf{k} \equiv -[\lim_{t\to0}(d/dt)\,g(\mathbf{k},t)]/g(\mathbf{k},0)$. The denominator $g(\mathbf{k},0)$ is the static structure factor given by

$$g(\mathbf{k},0) = L\mathbf{s}^\mathrm{T}\Phi^{-1}\mathbf{s} \tag{27}$$

As regards the numerator, it is evident that

$$\lim_{t\to0}(d/dt)\,[\mathbf{U}\exp(-\Lambda t)\mathbf{U}^{-1}] = -\mathbf{U}\Lambda\mathbf{U}^{-1} = -\Omega$$

Therefore we have an expression for $\Gamma_\mathbf{k}$ without any detailed information on Λ and $\mathbf{U}$:

$$\Gamma_\mathbf{k} = (\mathbf{s}^\mathrm{T}\Theta\mathbf{s})/(\mathbf{s}^\mathrm{T}\Phi^{-1}\mathbf{s}) \tag{28}$$

From eq 15 and 28, we easily have an expression for the apparent diffusion coefficient $\Gamma_\mathbf{k}/k^2$ as

$$\Gamma_\mathbf{k}/k^2 = [D_\mathrm{G} + (L^2/12)D_rf_1(K) - (D_\parallel - D_\perp)\{1/3 - f_2(K)\}]A(kL,\nu) \tag{29}$$

where

$$A(kL,\nu) \doteq (\mathbf{s}^\mathrm{T}\mathbf{s})/(\mathbf{s}^\mathrm{T}\Phi^{-1}\mathbf{s}) \tag{30}$$

$$f_1(K) = (3/K^2)(\mathbf{s}^{\mathrm{T}}\mathbf{R}\mathbf{s})/(\mathbf{s}^{\mathrm{T}}\mathbf{s}) \tag{31}$$

$$f_2(K) = (\mathbf{s}^{\mathrm{T}}\mathbf{T}\mathbf{s})/(\mathbf{s}^{\mathrm{T}}\mathbf{s}) \tag{32}$$

and K is defined in eq 11. The square of the vector $\mathbf{s}$,$\mathbf{s}^{\mathrm{T}}\mathbf{s}$, equals the particle structure factor[5] $S(kL) \equiv \sum_{\mathrm{even}\,l}(2l + 1)b_l(K)^2$. The quantity $A(kL,\nu)$ expresses the ratio of $\Gamma_{\mathbf{k}}$ to that of zero polymer concentration, if $D_{\parallel}$, $D_{\perp}$, and D_{r} do not depent on the rod concentration ν. Since $\mathbf{\Phi} = \mathbf{E}$ at $\nu = 0$, it is evident that $A(kL,0) = 1$. Equation 29 with $A(kL,0) = 1$ agrees with the one previously given,[2] where $f_1(K)$ and $f_2(K)$ are also tabulated. Limiting values of $f_1(K)$ and $f_2(K)$ at $K \to 0$ and $K \to \infty$ are $f_1(0) = 0$, $f_1(\infty) = 1$, $f_2(0) = {}^1/_3$, and $f_2(\infty) = 0$.

3. Numerical Methods

3.1. Representations of the Vector s and Matrices in a Computer Program. So far, subscripts of the elements of the column vector $\mathbf{s}$ and various matrices that appear in eq 26 are assumed to run from zero to infinity. However, it is out of the question that when we translate the equation into a computer program, we have to truncate the subscript value at some "sufficiently" large integer N. But, how large must N be to be "sufficiently" large? In relation to this question, there is one thing to be noted, i.e., the way in which we construct the vector $\mathbf{s}$ and relevant matrices.

It is important to notice that we can neglect the odd-subscript elements of the vector and matrices in eq 26. Suppose we already know an even value of N. Then, we construct the column vector $\mathbf{s}$ as

$$\mathbf{s} = (s_0, s_2, s_4, ..., s_N)^{\mathrm{T}} \tag{33}$$

and a matrix $\mathbf{M}$, which represents any of the matrices in eq 26, as

$$\mathbf{M} = \begin{pmatrix} M_{0,0} & M_{0,2} & \dots & M_{0,N-2} & M_{0,N} \\ M_{2,0} & M_{2,2} & \dots & M_{2,N-2} & M_{2,N} \\ \vdots & \vdots & & \vdots & \vdots \\ M_{N,0} & M_{N,2} & \dots & M_{N,N-2} & M_{N,N} \end{pmatrix} \tag{34}$$

The reason for completely leaving out odd-subscript elements from the vector and matrices is because matrix elements of $\mathbf{\Theta}$ and $\mathbf{W}$ having subscripts with mixed parity are all zero, as shown in eq 15–18 and eq 22–24. This fact guarantees that there is no coupling between even- and odd-subscript elements of $\mathbf{s}$ after multiplication of the matrices to the vector $\mathbf{s}$ from the left. Since only the even-subscript elements of $\mathbf{s}$ contribute to $g(\mathbf{k}, t)$ (cf. eq 9), we can completely neglect odd-subscript elements from the vector and matrices in eq 26. Note that the actual size of $\mathbf{M}$ is $[(N/2) + 1, (N/2) + 1]$, but we still use the N value to denote the size of the matrices.

Armed with these mathematical considerations, we can answer the question posed above about the appropriate value of N. In the case of a dilute solution, this question has been already answered:[2] When $\nu = 0$, we solve the eigenvalue problem for $\mathbf{\Theta}$, because $\mathbf{\Omega} = \mathbf{\Theta}$. Let N' be the smallest even integer that satisfies $(2N' + 1)b_{N'}(K)^2 \le 10^{-6}\mathbf{s}^{\mathrm{T}}\mathbf{s}$. Then, $N = 2N'$ is large enough to give N independent eigenvalues λ_p of $\mathbf{\Theta}$ for $p \le N'$. With this N value, we can compute $g(\mathbf{k}, t)$ with high accuracy, i.e., within a relative error of 10^{-6}. During the course of this study, we found that this N value is also large enough to give N independent eigenvalues λ_p of $\mathbf{\Omega}$ for the reasonable concentration range of $0 \le \nu \le \nu^*$, where ν^* ($\equiv 16/\pi bL^2$) is the characteristic concentration above which the isotropic phase becomes unstable.[6] The reason why this N value is valid also for the semidilute case is because the contribution of matrix $\mathbf{W}$ to matrix $\mathbf{\Phi}$ ($= \mathbf{E} + \pi\nu bL^2\mathbf{W}$) is always limited to the upper left corner of the matrix. When $kL \ll 1$, matrix $\mathbf{\Phi}$ almost equals $\mathbf{E}$ except $\mathbf{\Phi}_{00}$, because all off-diagonal elements of $\mathbf{W}$ are negligibly small, and the magnitude of the diagonal ones decreases as $\mathbf{W}_{nn} \simeq O(1/n^2)$. When $kL \ge 40$, the relation $\mathbf{\Phi} \approx \mathbf{E}$ holds fairly well, because the order of magnitude of the every element of $\mathbf{W}$ is smaller than 0.005. (See also eq A.2). In the intermediate region of kL, elements of $\mathbf{W}$ larger than 0.01 are confined to the upper left region of $\mathbf{W}$, the size of which is smaller than 5×5. These properties of $\mathbf{\Phi}$ ensure that only the lowest few eigenvalues of $\mathbf{\Omega}$ are affected even in the highest concentration range. The N value determined by $N = 2N'$ is large enough to give N independent eigenvalues λ_p of $\mathbf{\Omega}$ for $p \le N'$ and $0 \le \nu \le \nu^*$.

3.2. Algorithms. We computed $g(\mathbf{k},t)$ and $\Gamma_{\mathbf{k}}$ on a 16-bit microcomputer equipped with an 80286 processor, 80287 math coprocessor, and 640K bytes of memory. Figure 1 shows the flowchart of our program, which is coded in FORTRAN77. The program computes $g(\mathbf{k},t)$ at delay times of 0 s and 1 μs to 0.5 s in steps of 1, 2, and 5, in total of 19 points. The time typically required for the calculation of 19 values of $g(\mathbf{k},t)$ at $kL = 4$ was less than 2 min on our microcomputer running at 8 MHz of clock speed.[7] The computation time increases for larger kL values. Another program, using the method of spline interpolation,[12] approximately recovers the profile of $g(\mathbf{k},t)$ from a table of $\ln\,[g(\mathbf{k},t)]$ computed as above. Using about 250K bytes of memory, we could solve the eigenvalue problem of the maximum size of $N = 160$ in double precision.

The following are the major subroutines in our program: To compute $j_l(x)$, we used DJSPHB,[8] which is based on the backward recurrence formula for $j_l(x)$ or Miller's device.[13] To compute $b_l(K)$, we used a formula[2] for the integration of $j_l(x)$

$$b_{l+2}(K) = \frac{l+1}{l+2}b_l(K) - \frac{2l+3}{l+2}j_{l+1}(K)/K \tag{35}$$

and the subroutine DSICI[8] that gives the sine integral $\mathrm{Si}(x) = \int_0^x \sin t/t\,\mathrm{d}t$. The subroutine RG[9] solves the eigenvalue problem for the real general matrix $\mathbf{\Omega}$ and outputs the eigenvalues λ_p for $p = 0, 2, ..., N$ and eigenvector matrix $\mathbf{U}$. DGECO and DGECI[11] together compute the inverse of matrices $\mathbf{U}$ and $\mathbf{\Phi}$.

3.3. Numerical Computation. In order to see the overall features of the present theory, we numerically computed $A(kL,\nu)$ and eigenvalues of $\mathbf{\Omega}$. The former shows how the initial decay rate is influenced by the rod–rod interaction, and the latter shows how the effect is distributed among various eigenmodes. Table I shows $A(kL,\nu)$ as a function of kL and ν/ν^*.

Note two points in Table I. (1) When the kL value is fixed, the ν dependence of $A(kL,\nu)$ is almost linear:

$$A(kL,\nu) = 1 + m(kL)\nu/\nu^* \tag{36}$$

The value of $m(kL)$ is smaller for larger kL values: $m(0) = 8$, $m(5) = 4.33$, $m(10) = 2.11$, and $m(15) = 1.39$. Table II shows $m(kL)$ as a function of kL. It is rather easy to show that $m(kL) = 8(\mathbf{s}^{\mathrm{T}}\mathbf{s}) - O(\{kL\}^4) - O(\nu/\nu^*)$; i.e., the kL dependence of $m(kL)$ is mainly determined by the $\mathbf{s}^{\mathrm{T}}\mathbf{s}$ term. (2) Though Table I includes only positive values of $A(kL,\nu)$, the $A(kL,\nu)$ value for $\nu/\nu^* \ge 1$ becomes suddenly negative within ±0.01 of a certain kL value. The negative $A(kL,\nu)$ is, of course, unphysical and corresponds to the fact that the isotropic phase is unstable at this concentration.

Table III shows eigenvalues of $\mathbf{\Omega}$ at $\nu/\nu^* = 0.1$ normalized by those at $\nu/\nu^* = 0.0$. We can see from Table III that only the lowest few eigenvalues are affected for $kL \le 20$

Table I
$A(kL,\nu)$ as a Function of kL and ν/ν^* ($\nu^* \equiv 16/\pi bL^2$)

		$A(kL,\nu)$ at ν/ν^* =						
kL	$\mathbf{s}^T\mathbf{s}$	0.01	0.02	0.05	0.1	0.2	0.5	1.0
1	0.9728	1.0778	1.1556	1.3891	1.7782	2.5563	4.8905	8.7682
2	0.8973	1.0717	1.1434	1.3585	1.7169	2.4336	4.5818	8.1255
3	0.7902	1.0628	1.1257	1.3141	1.6281	2.2556	4.1326	7.2110
4	0.6724	1.0528	1.1057	1.2641	1.5279	2.0548	3.6278	6.2039
5	0.5627	1.0433	1.0866	1.2164	1.4326	1.8641	3.1519	5.2671
6	0.4727	1.0354	1.0708	1.1771	1.3540	1.7072	2.7627	4.5050
7	0.4056	1.0297	1.0594	1.1484	1.2967	1.5931	2.4796	3.9480
8	0.3577	1.0258	1.0517	1.1292	1.2583	1.5162	2.2878	3.5663
9	0.3228	1.0232	1.0464	1.1160	1.2318	1.4633	2.1552	3.3001
10	0.2949	1.0211	1.0423	1.1056	1.2111	1.4218	2.0516	3.0927
11	0.2705	1.0193	1.0386	1.0963	1.1926	1.3849	1.9597	2.9104
12	0.2487	1.0176	1.0351	1.0878	1.1756	1.3510	1.8756	2.7446
13	0.2296	1.0161	1.0322	1.0804	1.1608	1.3213	1.8020	2.5994
14	0.2135	1.0149	1.0297	1.0743	1.1486	1.2970	1.7415	2.4795
15	0.2001	1.0139	1.0278	1.0694	1.1388	1.2776	1.6929	2.3826

Table II
$m(kL)$ as a Function of kL

kL	$m(kL)$	kL	$m(kL)$	kL	$m(kL)$	kL	$m(kL)$
0.0	8.00000						
1.0	7.78150	11.0	1.92606	21.0	0.98833	31.0	0.66807
2.0	7.16915	12.0	1.75616	22.0	0.94498	32.0	0.64614
3.0	6.28106	13.0	1.60758	23.0	0.90520	33.0	0.62600
4.0	5.27906	14.0	1.48584	24.0	0.86705	34.0	0.60771
5.0	4.32547	15.0	1.38844	25.0	0.83053	35.0	0.59076
6.0	3.53950	16.0	1.30677	26.0	0.79678	36.0	0.57449
7.0	2.96749	17.0	1.23247	27.0	0.76664	37.0	0.55860
8.0	2.58265	18.0	1.16195	28.0	0.73978	38.0	0.54326
9.0	2.31816	19.0	1.09632	29.0	0.71500	39.0	0.52888
10.0	2.11093	20.0	1.03816	30.0	0.69119	40.0	0.51562
						∞	0.00000

Table III
Normalized Eigenvalues of Ω at $\nu/\nu^* = 0.1$

	mode number					
kL	0	2	4	6	8	10
0.2	1.79911	0.90018	0.98752	0.99610	0.99829	0.99910
2.0	1.71593	0.91715	0.98932	0.99668	0.99855	0.99924
20.0	1.03369	1.01024	1.01967	1.02933	1.00554	0.99970

by the mean-field potential **W**. At $kL = 0.2$, normalized eigenvalue $\lambda_p/\lambda_{p,0}$ initially wiggles around 1.0 and approaches unity with increasing mode number p, and for higher kL values, the amplitude of the wiggling becomes smaller. This wiggling behavior does not come from the translational–rotational coupling, but from the structure of matrix **W** itself, because, even when we put $D_\parallel = D_\perp$, the results are not much different from those in Table III.

From these results, it is clear that the mean-field hard-rod interaction potential affects only the spatially long and temporarily slow modes of fluctuations in the solution. This is a natural consequence of the form of the interaction potential $W_\mathbf{k}(\mathbf{u},\mathbf{u}')$ given in eq 8. The $|\mathbf{u} \times \mathbf{u}'|$ term in $W_\mathbf{k}(\mathbf{u},\mathbf{u}')$ is proportional to the probability that two rods with orientation $\mathbf{u}$ and $\mathbf{u}'$ collide with each other. The $s_\mathbf{k}(\mathbf{u})$ and $s_\mathbf{k}(\mathbf{u}')$ terms express the weights of the collision to be "seen" in scattering experiments. When kL is large, only the collision of two rods, both of which are perpendicular to $\mathbf{k}$, contributes to $W_\mathbf{k}(\mathbf{u},\mathbf{u}')$, but the ratio of such collision in the whole collisional events is small. The weight terms $s_\mathbf{k}(\mathbf{u})$ and $s_\mathbf{k}(\mathbf{u}')$ make the effect of the potential $W_\mathbf{k}(\mathbf{u},\mathbf{u}')$ weak on higher eigenmodes and/or for large kL.

4. Discussion

In order to clarify the implications of the DSO theory, we first discuss the concentration dependence of $\Gamma_\mathbf{k}/k^2$.

4.1. Concentration Dependence of Γ_k/k^2 at $\mathbf{k} = 0$.

In this section, we summarize the classical theory of the concentration dependence of the mutual diffusion coefficient $^*D_\mathrm{G}$, the value of which we obtain by extrapolating to $\mathbf{k} = 0$ the apparent diffusion coefficient $^*D_\mathbf{k} \equiv \Gamma_\mathbf{k}/k^2$ measured by the dynamic light scattering method.

The mutual diffusion coefficient $^*D_\mathrm{G}$ is dependent on the polymer concentration:[14]

$$^*D_\mathrm{G} = \frac{k_\mathrm{B}T}{\zeta_0}(1 - \bar{v}_2c)(1 + 2A_2Mc + ...)/(1 + k_\zeta c + ...) \tag{37}$$

where c is the weight concentration of the polymer, ζ_0 the zero concentration friction coefficient, $\bar{v}_2$ the specific volume of polymer of molecular weight M, A_2 the osmotic second virial coefficient, and the factor $(1 + k_\zeta c + ...)$ expresses the change in friction due to direct physical hindrance and/or hydrodynamic interaction. The superscript * of $^*D_\mathrm{G}$ denotes that this quantity includes the thermodynamic interaction term $(1 + 2A_2Mc + ...)$.

We have no theory that successfully predicts the strength of k_ζ. Though a theoretical expression[16] for k_ζ is available

$$k_\zeta = (\zeta_0/3\eta)(3A_2N_\mathrm{A}^{1/2}/2\pi)^{2/3}M^{1/3} \tag{38}$$

where η is the solvent viscosity, a comparison of eq 38 with sedimentation and light-scattering data of α-helical polypeptides[17] revealed that this equation was valid only qualitatively. Doi and Edwards[18] (the DE theory) estimated the diffusion coefficients of rodlike polymers in the strongly entangled state as

$$D_\parallel \simeq D_{\parallel,0}, \quad D_\perp \simeq 0, \quad D_\mathrm{r} \simeq D_{\mathrm{r},0}(\nu L^3)^{-2} \tag{39}$$

Equation 39 was expected to work in the concentration range of $1 \ll \nu L^3 \ll L/b$, but the observed data for D_r seems to be fitted by an empirical equation[19,20]

$$D_\mathrm{r} = D_{\mathrm{r},0}/[1 + \beta(\nu L^3)^2] \tag{40}$$

where β is a constant of the order of 10^{-3}. A precise evaluation of the concentration dependence of the $D_\parallel$, $D_\perp$, and D_r values has been done neither on the whole nor individually.

Though the friction coefficient ζ may be written as

$$\zeta = \zeta_0(1 + k_\zeta c + ...) \tag{41}$$

the linear approximation with respect to c is not valid when the polymer concentration is high. We shall consider hereafter the friction coefficient ζ as a function of the polymer concentration c, the approximate form of which is given by eq 41 valid only when c is low.

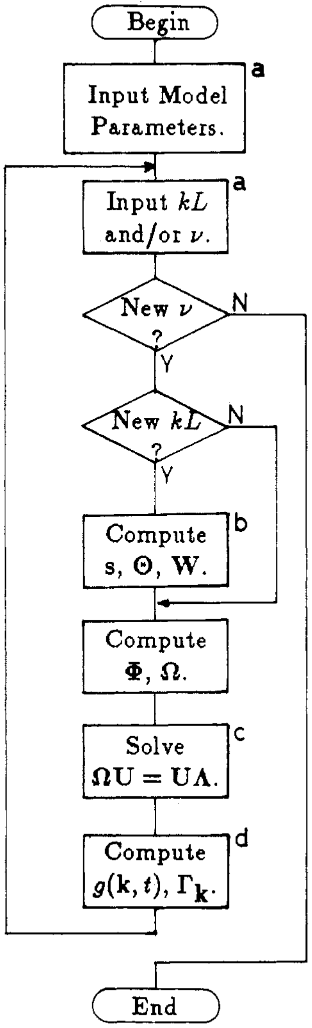

Figure 1. Flowchart of the numerical computation of eq 26. Notes and comments: All computations were done in double precision. (a) Model parameters are L, b, $D_\perp$, $D_\parallel$, D_r, kL, and ν. (b) To compute **s**, we used the subroutines DJSPHB and DSICI[8] that compute $j_l(x)$ and $\int_0^x \sin t/t \, dt$, respectively. To compute the eigenvalues of the real symmetrical tridiagonal matrix **Φ**, we used the subroutine IMTQL1.[9] To compute matrix **W**, we used the subroutine CLEBSH that computes the C coefficient $C(l_1l_2l_3;000)$ (eq 14). (c) To solve the eigenvalue problem for matrix **Ω**, we used the subroutine RG.[9] Since RG returns the real part of the eigenvalues not exactly sorted, we used an indexing subroutine INDEXX to sort the eigenvalues exactly in the ascending order.[10] Though matrix **Ω** is in general nonsymmetrical for $\nu > 0$, we have not obtained complex eigenvalues so far. To compute the inverse of matrices **U** and **Φ**, we used the subroutines DGECO and DGECI.[11] (d) We computed $g(\mathbf{k},t)$ at delay times of 0 s and 1 μs to 0.5 s in steps of 1, 2, and 5. PCUBIC and PSPLINE[12] recovered and approximated the value of $g(\mathbf{k},t)$ at an arbitrary value of $t \leq 0.5$ s from a table of ln $[g(\mathbf{k},t)]$ computed as above.

It should be noted that when we apply eq 37 to a rigid-rod suspension, we have to replace the frictional term k_BT/ζ with an average of the lengthways and sideways components:

$$*D_G = D_G(1 + 2A_2Mc + ...) \tag{42}$$

$$D_G = \left[\frac{1}{3}\left(\frac{k_BT}{\zeta_\parallel}\right) + \frac{2}{3}\left(\frac{k_BT}{\zeta_\perp}\right)\right](1 - \bar{v}_2c) \tag{43}$$

The $(1 - \bar{v}_2c)$ term in eq 43 is almost equal to 1 in the present case, because

$$\bar{v}_2c = \bar{v}_2(M/N_A)\nu = (\pi/4)\nu b^2L \leq (\pi/4)\nu^* b^2L = 4b/L \ll 1$$

where we assumed that the polymer is a solid rod with no solvation.

We express the concentration dependence of $*D_G$ as

$$*D_G = D_{G,0}(1 + k_Dc + ...) \tag{44}$$

Since we do not know the functional form of $\zeta_\parallel(c)$ and $\zeta_\perp(c)$, we use eq 41 to discuss the strength of k_D. Using eq 41 and ignoring terms of order c^2 or higher, we have a relationship between parameters k_D, $2A_2M$, $\bar{v}_2$, and k_ζ given by

$$k_D = 2A_2M - \bar{v}_2 - k_\zeta \tag{45}$$

where k_ζ is the weighted average of $k_{\zeta,\parallel}$ and $k_{\zeta,\perp}$:

$$k_\zeta = [(1/3)D_{\parallel,0}k_{\zeta,\parallel} + (2/3)D_{\perp,0}k_{\zeta,\perp}]/D_{G,0} \tag{46}$$

So far, our discussion is limited to $\mathbf{k} = 0$. Therefore eq 37–46 are valid only at $\mathbf{k} = 0$.

4.2. Concentration Dependence of $\Gamma_{\mathbf{k}}/k^2$ for Arbitrary k. Now we will show that eq 29 is a generalization of eq 42 for arbitrary values of **k**. From eq A.6, we have an approximated form of $A(k,\nu)$ at $\mathbf{k} \to 0$ and $\nu \to 0$ as

$$\lim_{\substack{\mathbf{k}\to 0 \\ \nu \to 0}} A(kL,\nu) = 1 + 2\left[\frac{\pi}{4}bL^2\frac{N_A}{M^2}\right]Mc$$

Since the osmotic second virial coefficient for a solid rod suspension[15] is given by $A_2 = (\pi/4)bL^2N_A/M^2$, we have

$$\lim_{\substack{\mathbf{k}\to 0 \\ \nu \to 0}} A(kL,\nu) = 1 + 2A_2Mc \tag{47}$$

The factor $A(kL,\nu)$ reduces to $(1 + 2A_2Mc + ...)$ at $\mathbf{k} \to 0$, but the factor $A(kL,\nu)$ itself is defined for arbitrary values of kL. Comparing eq 36 and 47, we generalize the osmotic second virial coefficient A_2 as a function of kL:

$$A(kL,\nu) = 1 + 2A_2(kL)Mc + ... \tag{48}$$

$$A_2(kL) = \frac{m(kL)}{m(0)}A_2 \tag{49}$$

Since $f_1(0) = 0$ and $f_2(0) = {}^1/_3$ in eq 29, we have the limiting form of eq 29 as

$$\lim_{\mathbf{k}\to 0} *D_{\mathbf{k}} = [(1/3)D_\parallel + (2/3)D_\perp](1 + 2A_2Mc + ...) \tag{50}$$

Equation 50 agrees with eq 42 with the definition of

$$D_i = \frac{k_BT}{\zeta_i}(1 - \bar{v}_2c) \tag{51}$$

where the value of the subscript i is "∥", "⊥", or "r". Note that diffusion coefficients used in the DE theory (eq 39) do not include the $A(kL,\nu)$ term and are the self-diffusivities given by eq 51.

We rewrite eq 29 as a weighted sum of diffusion coefficients:

$$*D_{\mathbf{k}} = W_\parallel {*D_\parallel} + W_\perp {*D_\perp} + W_r(L^2/12){*D_r} \tag{52}$$

where $*D_i$ for i = "∥", "⊥", "r" are $D_\parallel A(kL,\nu)$, $D_\perp A(kL,\nu)$, $D_rA(kL,\nu)$, respectively. The weights W_i for i = "∥", "⊥", "r" are $f_2(K)$, $\{1 - f_2(K)\}$, $f_1(K)$, respectively. Each $*D_i$ is dependent on the polymer concentration and is expressed by an equation similar to eq 37:

$$*D_i = \frac{k_BT}{\zeta_i}(1 - \bar{v}_2c)A(kL,\nu) \tag{53}$$

The $(1 - \bar{v}_2c)$ and $A(kL,\nu)$ terms are common to all $*D_i$'s, but the ζ_i term is not.

In analogy with eq 44, we write

$$^{*}D_{\mathbf{k}} = D_{\mathbf{k},0}\{1 + k_{\mathrm{D}}(kL)c + ...\} \qquad (54)$$

where the parameter k_{D} is a function of kL.

At first, we discuss the initial portion of the concentration dependence of $^{*}D_{\mathbf{k}}$, where the linear approximation with respect to c is valid for eq 41. Discussion on the strength of $k_{\mathrm{D}}(kL)$ can be done similarly to the one previously made for k_{D}. Using eq 41 and ignoring terms of order c^2 or higher, we have a relationship for $k_{\mathrm{D}}(kL)$ as

$$k_{\mathrm{D}}(kL) = 2A_2(kL)M - \bar{v}_2 - k_{\zeta}(kL) \qquad (55)$$

where $k_{\zeta}(kL)$ is the weighted average of $k_{\zeta,i}$:

$$k_{\zeta}(kL) = [W_{\parallel}D_{\parallel,0}k_{\zeta,\parallel} + W_{\perp}D_{\perp,0}k_{\zeta,\perp} + W_{\mathrm{r}}(L^2/12)D_{\mathrm{r},0}k_{\zeta,\mathrm{r}}]/D_{\mathbf{k},0} \qquad (56)$$

The quantity $k_{\zeta}(kL)$ depends on kL, because the weights W_i's are functions of kL. Note that $k_{\mathrm{D}}(kL)$ is a decreasing function of kL, because (i) $A_2(kL)$ is a decreasing function of kL as shown in eq 49 and (ii) $k_{\zeta}(kL)$ is expected to be an increasing (or, at least, nondecreasing) function of kL. The latter point can be easily seen, if we note

$$k_{\zeta}(0) = (k_{\zeta,\parallel} + k_{\zeta,\perp})/2 \qquad k_{\zeta}(\infty) = (k_{\zeta,\perp} + k_{\zeta,\mathrm{r}})/2$$

where we assumed a relationship $0.5D_{\parallel,0} = D_{\perp,0} = (L^2/12)D_{\mathrm{r},0}$ for the long rod limit. Since the relation $k_{\zeta,\parallel} \leq (k_{\zeta,\perp}$ and $k_{\zeta,\mathrm{r}})$ is likely to hold, the function $k_{\zeta}(kL)$ would be an increasing function of kL. Even when $k_{\zeta,i}$ are all equal, the function $k_{\zeta}(kL)$ is constant irrespective of the kL value. Other cases, such as $k_{\zeta,\parallel} \geq (k_{\zeta,\perp}$ and $k_{\zeta,\mathrm{r}})$, are unlikely.

Next, we consider the $^{*}D_{\mathbf{k}}$ value when the polymer concentration is high. Even when c is high, the linear approximation for the $A(kL,\nu)$ term with respect to c is valid (cf. eq 36). If the linear approximation is also valid for all ζ_i when c is high, $^{*}D_{\mathbf{k}}$ would finally reach a constant level of $D_{\mathbf{k},0}2A_2(kL)M/k_{\zeta}(kL)$, where we set the $(1 - \bar{v}_2c)$ term to unity. If all ζ_i are to be approximated with polynomials of order $n \geq 2$ for high c, the $^{*}D_{\mathbf{k}}$ value would decrease to zero when c is high. When $2A_2(kL)M > k_{\zeta}(kL)$ in this case, $^{*}D_{\mathbf{k}}$ would go through a maximum and then decrease with increasing concentration. If the linear approximation is valid for one of ζ_i, but others are approximated with polynomials of order n higher than one, $^{*}D_{\mathbf{k}}$ would eventually reach a constant level higher than zero with increasing c. Whether $^{*}D_{\mathbf{k}}$ goes through a maximum before reaching the constant level would depend on the relationship of the magnitude of the $2A_2(kL)M$ and $k_{\zeta,i}$ terms. When reliable data of $^{*}D_{\mathbf{k}}$ are available for a wide range of the polymer concentration, the above consideration will serve as a guide to interpreting the concentration dependence of $^{*}D_{\mathbf{k}}$.

4.3. Concentration Dependence of Each $D_{\parallel}$, $D_{\perp}$, and D_{r}. It should be pointed out that by use of eq 52 (or eq 55 when linear approximation with respect to c is valid), we have the possibility of studying the concentration dependence of each D_i. Suppose we have DLS data for rod suspensions in a wide range of concentrations and scattering angles. Since the functional forms of W_i and $A(kL,\nu)$ in eq 52 are known, it is possible to determine the concentration dependence of D_i separately. Data analysis would proceed as follows: (i) Since the contribution of $^{*}D_{\parallel}$ to $^{*}D_{\mathbf{k}}$ is small when $kL \geq 10$ (cf. Table I of ref 2) and the kL dependence of $A(kL,\nu)$ is weak for $kL \geq 10$, the $D_{\perp}$ and D_{r} values would at first be determined by using data at different scattering angles in this kL region; (ii) next, the $D_{\parallel}$ value would be estimated, by using the data for $kL \leq 10$; and (iii) after repeating steps i and ii several times, reasonable values for $D_{\parallel}$, $D_{\perp}$, and D_{r} would be estimated. When the data for $kL \geq 10$ are not available, the situation would be a little more complicated because of the simultaneous contribution of the three diffusion coefficients and the stronger kL dependence of the $A(kL,\nu)$ term, but data analysis would be still possible. Comparison of computed and observed correlation function profiles would also be useful in judging the consistency of the estimated parameters.

4.4. Comparison with Experimental Observations. We shall compare the DSO theory with experimental data for poly(γ-benzyl L-glutamate) (PBLG)[21] and fd virus.[22,23] Our discussion is rather qualitative, because real macromolecules, such as PBLG and fd virus, are more or less flexible, but the theory assumes the polymer to be a perfectly rigid rod. The comparison, however, will be useful to our understanding of the implications of the theory, and it will also give us some hints on how to interpret the DLS spectrum of rodlike polymers in less dilute solutions.

Russo, Karasz, and Langley[21] extensively studied solutions of PBLG in N,N-dimethylformamide (DMF) in a very wide concentration range ($4 < \nu L^3 < 1500$ or $0.04 < \nu bL^2 < 15$) using the dynamic light scattering technique. We briefly summarize their work here.

1. Physicochemical parameters for one of their samples are $M = 3.0 \times 10^5$ Da (Da = dalton), $\bar{v}_2 = 0.791$ cm^3/g, and $L = 205.5$ nm.
2. The virial coefficient, measured with the static light scattering method, is $A_2 = 3.1 \times 10^{-4}$ (cm^3 mol)/g^2, which is within 3% of the excluded-volume limit ($=3.2 \times 10^{-4}$ (cm mol)/g^2) calculated for a rod of geometric (as opposed to hydrodynamic) diameter $b_{\mathrm{g}} = 1.4$ nm.[24]
3. The D_{G} value extrapolated to infinite dilution is within 10% of the value predicted by the Kirkwood–Riseman[25] or Broersma[26] equations, with hydrodynamic diameter $b_{\mathrm{h}} = 2$ nm.
4. The apparent diffusion coefficient $^{*}D_{\mathbf{k}}$ increases with concentration, but the increase is weaker at higher θ than at lower θ (cf. Figure 10 of ref 21), where θ is the scattering angle. The k_{D} value at $\theta = 90°$ ($kL \simeq 4.0$) is 11 cm^3/g.
5. Though the initial decay rate $\Gamma_{\mathbf{k}}$ increases with concentration, the correlation function has a slow tail when $\nu L^3 \geq 100$; i.e., high concentration correlation functions become extremely nonexponential.
6. Russo et al. concluded that k_{ζ} was a decreasing function of the concentration c (cf. Figure 9 of ref 21). The average of $k_{\zeta}(c)$ applicable to most of the measured concentration regime was $k_{\zeta} = 174$ cm^3/g. They further computed $D^{\mathrm{I}} \equiv D_{\mathbf{k},0}(1 - \bar{v}_2c)/(1 + k_{\zeta}(c)c)$ and showed that for $\nu L^3 \geq 100$, the D^{I} value decreased below $(1/2)D_{\mathbf{k},0}$, the lower limit of the prediction of the DE theory. They ascribed the smallness of the D^{I} value to filament flexibility and finite diameter.

The fd virus is a semiflexible filamentous virus, the physicochemical properties of which are well characterized.[27] We studied the DLS spectrum of the virus suspensions in dilute and semidilute regimes.[22,23] Summary of experimental data is as follows:

1. Physicochemical parameters for the fd virus are $M = 1.64 \times 10^7$ Da, $\bar{v}_2 = 0.720$ cm^3/g, and $L = 895$ nm.[27]
2. The virial coefficient is $A_2 = 0.97 \times 10^{-5}$ (cm^3 mol)/g^2, which gives the geometric diameter $b_{\mathrm{g}} = 6.8$ nm.[28,29]
3. The hydrodynamic diameter estimated from the $D_{\mathrm{G},0}$ and $D_{\mathrm{r},0}$ values is $b_{\mathrm{h}} = 9$ nm.[27]
4. The apparent diffusion coefficient $^{*}D_{\mathbf{k}}$ slightly increases with concentration at $\theta = 10.3°$ but decreases when $\theta \geq 30°$. The k_{D} value is 31.7 cm^3/g at $\theta = 10.3°$ ($kL = 2.75$) but -98.3 cm^3/g at $\theta = 90°$ ($kL = 22$).[30] The k_{ζ} value is 225 cm^3/g.[27]
5. A long tail of the correlation function appears with the increase of the virus concentration.[22]

6. Using the values of $^*D_{\mathbf{k}}$ at $\theta = 10.3°$ for various virus concentrations as the concentration-dependent translational diffusion coefficient $^*D_G$, Fujime et al.[23] evaluated $^*D_\parallel$ and $^*D_\perp$. Following the DE treatment, they introduced an adjustable parameter β (≤ 1) to reduce the rotational diffusion coefficient at high concentration. Using the values of $^*D_\parallel$, $^*D_\perp$, and $\beta D_{r,0}$, they simulated the $\Gamma_{\mathbf{k}}/k^2$ versus k^2 relationships and could obtain satisfactory results over the entire range of k^2 and virus concentrations studied so far. In order to interpret the long tail of the correlation function, they introduced a translational diffusion coefficient D_L at a long-t region, based on an analogy with Pusey's expression of $g(\mathbf{k},t)$ for a concentrated suspension of highly charged spheres strongly interacting with each other.[31]

We can learn much from these experimental observations and efforts to interpret DLS data.

1. The DSO theory assumes the polymer to be a solid rod. If a theory based on such mechanical considerations is to apply to macromolecular solutions, models of the solutions must be constructed in which the polymers appears as solid particles.[32] In this respect, care must be taken in choosing the value of the rod diameter b. The b value included in matrix Φ should be the geometrical diameter b_g that gives the correct A_2 value at $\mathbf{k} = 0$. Likewise, the zero concentration friction constant ζ_0 in eq 37 should use the hydrodynamic diameter b_h. The b value computed from $\bar{v}_2 = (\pi/4)b^2L(N_A/M)$ is 1.6 nm for PBLG and 5.3 nm for fd virus, which are different from both b_g and b_h values of these polymers.

2. The k_D value of both PBLG and fd virus is smaller at larger scattering angle. This behavior qualitatively agrees with our postulate that the function $k_D(kL)$ is a decreasing function of kL.

Let us consider the case of fd virus. The value of $2A_2(kL)M$ at $\theta = 10.3°$ ($kL = 2.75$) is *not* equal to $2A_2M = 2(0.97 \times 10^{-5})(1.64 \times 10^7) = 318.2$ but $(6.51/8)318.2 = 258.9$, because $m(kL)$ at $kL = 2.75$ is 6.51. Using the values of 258.9, 31.7, and 0.720 cm^3/g, respectively, for $2A_2(kL)M$, $k_D(kL)$, and $\bar{v}_2$ at $\theta = 10.3°$, we have $k_\zeta = 226.5$ cm^3/g. This k_ζ value is very close to the observed k_ζ value (=225 cm^3/g). If the fd virus were perfectly rigid, we would observe a smaller $\Gamma_{\mathbf{k}}/k^2$ value at $kL = 22$ without contribution of the bending modes, and this would further decrease the k_D value from -98.3 to roughly -135 cm^3/g. Using eq 55, we can interpret this large decrease of the k_D value from 31.7 cm^3/g (at $kL = 2.75$) to -135 cm^3/g (at $kL = 22$) as the decrease of the $2A_2(kL)M$ term. In fact, since $m(kL)$ at $kL = 22$ is 0.945, the value of $2A_2(kL)M$ at $kL = 22$ is $(0.945/8)318.2 = 37.6$. The decrease of the $2A_2(kL)M$ term from 258.9 to 37.6 exceeds that of the k_D term. Since our theory assumes perfectly rigid rods, while the virus is semiflexible, more detailed comparison would be inappropriate, but the above consideration strongly suggests the necessity to generalize the osmotic virial coefficient A_2 as a function of kL (and possibly the filament flexibility).

3. When $kL \leq 4$, the $2A_2(kL)M$ thermodynamic term in eq 55 just slightly exceeds the $(k_\zeta(kL) + \bar{v}_2)$ term, accounting for the modest increase in the apparent diffusion coefficient $^*D_{\mathbf{k}}$. For larger kL, $^*D_{\mathbf{k}}$ does decrease with concentration, because the $2A_2(kL)M$ term decreases with the increase of kL, while the $(k_\zeta(kL) + \bar{v}_2)$ term remains constant or increases. In order to see the consequence of this fact, we simulated the effect of concentration increase on the correlation function profiles, taking as an example a hypothetical rod of the size of the PBLG used by Russo et al. The simulation procedure is as follows. (1) We use physicochemical parameters of the PBLG for the hypothetical rod. (2) Since we do not know the individual $k_{\zeta,i}$ value for the PBLG, we adopt the simplest assumption: All $k_{\zeta,i}$ are equal, and k_ζ is not dependent on kL. (3) Using $m(4) = 5.279$ and the values of 186, 11, and 0.791 cm^3/g for $2A_2M$, $k_D(kL)$, and $\bar{v}_2$ respectively, we have $k_\zeta = 111$ cm^3/g. We evaluate the D_i values for several polymer concentrations with eq 51. (4) Using eq 26, we compute $g(\mathbf{k},t)$ for several scattering angles.

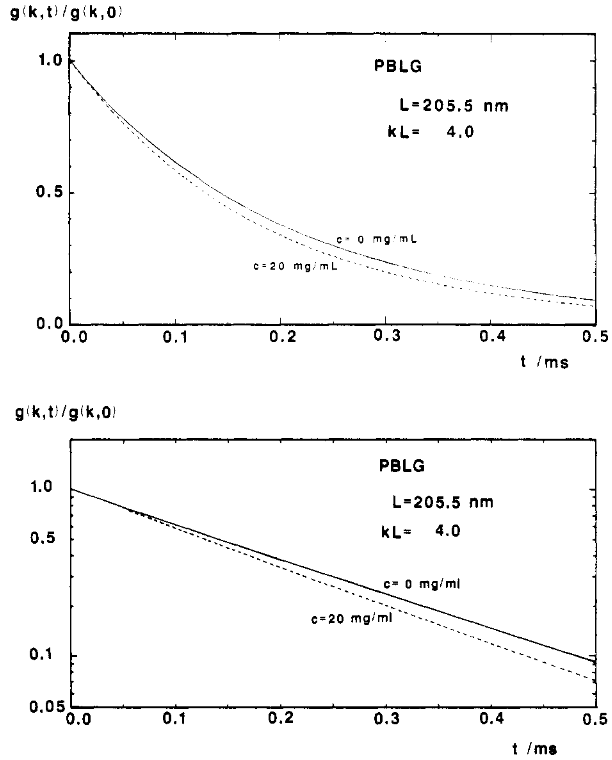

Figure 2. (a, Top) Profiles of simulated correlation functions $g(\mathbf{k},t)/g(\mathbf{k},0)$ for suspensions of hypothetical rods of the size of the PBLG used by Russo et al. (b, Bottom) In semilogarithmic form. Parameter values used are $L = 205.5$ nm, $D_{\mathbf{k},0} = 1.33 \times 10^{-7}$ cm^2/s, $kL = 4$, $m(kL) = 5.279$, $\bar{v}_2 = 0.791$ cm^3/g, and $k_\zeta = 111$ cm^3/g. Using Broersma's equation with $b_h = 2$ nm, we computed the $D_{i,0}$ values as $D_{G,0} = 1.25 \times 10^{-7}$ cm^2/s, $D_{\parallel,0} = 1.67 \times 10^{-7}$ cm^2/s, $D_{\perp,0} = 1.05 \times 10^{-7}$ cm^2/s, and $(L^2/12)D_{r,0} = 0.774 \times 10^{-7}$ cm^2/s. Upper curve: $c = 0$ mg/mL ($\nu L^3 = 0$). Lower curve: $c = 20$ mg/mL ($\nu L^3 = 348$). ($\nu L^3 = 17.4c$ and $\nu/\nu^* = 2.397 \times 10^{-2}c$ with c in mg/mL.) See details in the text.

Figure 2 shows profiles of the simulated correlation function $g(\mathbf{k},t)/g(\mathbf{k},0)$ at $kL = 4$. It is clear that at $kL = 4$, the correlation function decays a little more *quickly* with the increase of the polymer concentration and shows no anomaly in the tail part even at $\nu L^3 = 350$, where Russo et al. observed a slow tail. When kL is small, the DSO theory with the simplest assumption for $k_{\zeta,i}$ does not predict the appearance of the slow tail of the correlation function for $\nu L^3 \geq 100$.

The maximum kL value experimentally accessible with the PBLG sample is $kL \simeq 5.5$ at $\theta = 150°$. Using eq 55 with $2A_2(5.5)M = (3.93/8)186 = 91.4$ cm^3/g, $\bar{v}_2 = 0.791$ cm^3/g, and $k_\zeta = 111$ cm^3/g, we have $k_D(kL) = 91.4 - 0.791 - 111 = -20.4$ at $kL = 5.5$. We expect that the dynamic light scattering spectrum of the PBLG sample at $kL = 5.5$ would decrease more *slowly* with increasing the concentration.

4. Kubota and Chu[33] studied PBLG of molecular weight $M = 26.8 \times 10^4$ (PBLG-A) and 9×10^4 (PBLG-B) Da in DMF using the dynamic light scattering method. They reported that $^*D_{\mathbf{k}}$ of PBLG-A for $kL < 2$ initially increased with increasing concentration, but approached a plateau when $\nu L^3 \geq 400$ (Figure 10 of ref 33). The $^*D_{\mathbf{k}}$ of PBLG-B,

on the other hand, behaved quite differently from that of PBLG-A, i.e., $^*D_{\mathbf{k}}$ at first increased, went through a maximum at $\nu L^3 \simeq 150$, then decreased, and reached a constant level when $\nu L^3 \geq 230$ (Figure 12 of ref 33). Russo et al.'s $^*D_{\mathbf{k}}$, however, linearly increased with the concentration up to $\nu L^3 = 1400$ (Figure 10 of ref 21). Though, having these conflicting data, we might be able to say something about the concentration dependence of $^*D_{\mathbf{k}}$ using a polynomial of various order for each ζ_i, it is too early to say any conclusive statement about the functional form of ζ_i valid for a wide range of the polymer concentration c.

5. Russo et al. did not take into account the kL dependence of $A_2(kL)$ and used $2A_2M = 2(3.1 \times 10^{-4})(3.0 \times 10^5) = 186$ cm^3/g for $kL = 4$ in eq 55. Since $m(4) = 5.279$, the $2A_2(kL)M$ term is, in the light of the theory presented herein, to be evaluated instead as $(5.279/8)186 = 123$ cm^3/g. As a consequence, they overestimated the k_ζ value. The prediction of the DE theory that the lower limit of the D_{G} value is $(1/2)D_{\mathrm{G},0}$ holds only at $kL = 0$. Russo et al. found that the D^{I} value decreased below $(1/2)D_{\mathbf{k},0}$ for both $kL = 1.5$ and 4. Application of the DE prediction is appropriate for $kL = 1.5$ but not for $kL = 4$, because the contribution of the rotational mode is negligible at $kL = 1.5$ but not at $kL = 4$. The weights W_i of $D_\parallel$, $D_\perp$, and $(L^2/12)D_{\mathrm{r}}$ at $kL = 4$ are *not* $^1/_3$, $^2/_3$, 0, but 0.221, 0.889, 0.189, respectively (cf. Table I of ref 2), and the lower limit of $D_{\mathbf{k}}$ is $(0.221 \times 2)/(0.221 \times 2 + 0.889 + 0.189) = 0.291$ times as large as the $D_{\mathbf{k},0}$ value, where we assumed a relationship $0.5D_{\parallel,0} = D_{\perp,0} = (L^2/12)D_{\mathrm{r},0}$ for the long-rod limit and put $(1 - \bar{v}_2c) = 1$.

In spite of these minor corrections to their analysis, the main point in their conclusion is still valid: In a good solvent the repulsive thermodynamic interactions among rodlike polymers are sufficiently strong to cause an *increase* in the measured mutual diffusion coefficient. We would like to add one sentence to their conclusion: For larger kL, however, the magnitude of the thermodynamic effect becomes smaller, and the measured apparent diffusion coefficient $\Gamma_{\mathbf{k}}/k^2$ can *decrease* with the concentration.

6. Fujime et al.[23] could fit the $\Gamma_{\mathbf{k}}/k^2$ versus k^2 relationships using $^*D_\parallel$, $^*D_\perp$, and $\beta D_{\mathrm{r}0}$ and could also fit the long tail in the correlation function profile by introducing another parameter D_{L}. Their $^*D$'s implicitly include the contribution of the $A(kL,\nu)$ term at $\theta = 10.3°$, and since they used these $^*D_i$ values over the entire range of the scattering angles, they also did not take into consideration the kL dependence of the $A(kL,\nu)$ term.

Their analyses were mainly done in the region $kL \geq 10$ and $\nu/\nu^* \leq 0.2$. In this kL region, the flexibility effect on the DLS spectrum fully appears, and we do not know whether our $A(kL,\nu)$ for a rigid-rod solution is applicable to this case. But if we accept the assumptions that $A(kL,\nu)$ for suspensions of semiflexible filaments may not be much different from that of rigid-rod suspensions and that the bending modes of the virus particles are not much affected by $A(kL,\nu)$, then we may think that in higher kL region, their $^*D$'s would also *decrease* with concentration, but the contribution of the bending modes to $\Gamma_{\mathbf{k}}/k^2$ would remain constant. If this is the case, their D_{L} and $\beta D_{\mathrm{r},0}$ would be the manifestation of the decrease of $D_\perp$ and D_{r} with the increase of the virus concentration. The DSO theory would explain (at least, partly) the appearance of a long tail in fd virus data for larger kL values.

5. Conclusion

We obtained an expression for the dynamical structure factor of a semidilute solution of rodlike polymers, which enables us to evaluate such quantities as the static structure factor, initial decay rate, and profile of the dynamic light scattering spectrum in the entire range of $\mathbf{k}$, t, and ν. It was shown that our theory is a natural extension of previous two theories; one is the theory of the dynamic light scattering of dilute suspensions of rigid rods, which is valid for arbitrary $\mathbf{k}$ and t but only at $\nu = 0$, and the other is the theory of the concentration dependence of the mutual diffusion coefficient, which is valid for arbitrary ν but only at $\mathbf{k} = 0$ and $t = 0$.

Results of numerical computation show that the mean-field hard-rod interaction potential affects only the spatially long and temporarily slow modes of fluctuation in the solution. The quantity $A(kL,\nu)$ is a generalization of the repulsive thermodynamic term $(1 + 2A_2Mc + ...)$, which successfully explains the angular dependence of k_{D}. When kL is small, the repulsive thermodynamic interactions among rodlike polymers in a good solvent are sufficiently strong to cause an *increase* in the apparent diffusion coefficient $\Gamma_{\mathbf{k}}/k^2$. When kL is large, however, the magnitude of the thermodynamic effect becomes small, and the apparent diffusion coefficient can *decrease* with the concentration.

The present analysis raises the possibility of studying the concentration dependence of $D_\parallel$, $D_\perp$, and D_{r}, individually. This possibility would open a new pathway to experimentally studying Doi and Edwards' guess that the self-diffusion coefficients of rodlike polymers in the strongly entangled state would be $D_\parallel \simeq D_{\parallel,0}$, $D_\perp \simeq 0$, and $D_{\mathrm{r}} \simeq D_{\mathrm{r},0}(\nu L^3)^{-2}$.

In order to apply the present theory to real polymers, it is highly desirable that we should extend the theory to semiflexible filaments. Efforts in this direction will appear in the near future.

Acknowledgment. I thank Professor Masao Doi for useful discussion, who kindly sent a preprint of ref 1. I also thank Dr. Satoru Fujime, who read the manuscript and gave useful comments. I am grateful to Professor Paul S. Russo, who corrected the author's misunderstanding to his work and suggested several improvements in the manuscript.

Appendix A. Matrix W at k → 0 and k → ∞

We shall consider here the asymptotic form of matrix $\mathbf{W}$ in the limit of $\mathbf{k} \to 0$ and $\mathbf{k} \to \infty$. Let $\mathbf{W}_0$ and $\mathbf{W}_\infty$ respectively be

$$\mathbf{W}_0 \equiv \lim_{\mathbf{k}\to 0} \mathbf{W}$$

$$\mathbf{W}_\infty \equiv \lim_{\mathbf{k}\to \infty} \mathbf{W}$$

It is easy to derive the form of matrix $\mathbf{W}$ at $\mathbf{k} \to 0$. Since $j_l(x) \simeq x^l/(2l + 1)!!$ for $x \to 0$, we have $b_l(K) \simeq K^l/(l + 1)(2l + 1)!!$ for $kL \ll 1$. Retaining only those terms in eq 23 which have $b_0(K)$, we have

$$\lim_{\mathbf{k}\to 0} \mathbf{P}_{lp} = \lim_{\mathbf{k}\to 0} b_0(K)C(p0l;000)^2\delta_{lp} = \delta_{lp}$$

where we used $C(l0l;000) = 1$. Matrix $\mathbf{P}$ becomes an identity matrix $\mathbf{E}$ in the limit $\mathbf{k} \to 0$. Therefore matrix $\mathbf{W}_0$ becomes diagonal and

$$\begin{aligned} \{\mathbf{W}_0\}_{pp} &= 1/2 && \text{if} \quad p = 0 \\ &= -\{\mathbf{Q}\}_{pp} && \text{if} \quad p = 2, 4, ... \end{aligned} \tag{A.1}$$

It is not so easy to evaluate matrix $\mathbf{W}_\infty$, but using a numerical method, we can show that $\mathbf{W}_\infty \simeq O(\{kL\}^{-2})$. Since $\lim_{\mathbf{k}\to\infty} j_0(ks) = (\pi/k)\delta(s)$, we have

$$\lim_{\mathbf{k}\to\infty} b_0(K) = \lim_{\mathbf{k}\to\infty} \frac{1}{L}\int_{-L/2}^{L/2} j_0(ks)\ \mathrm{d}s = \frac{\pi}{kL}$$

Using eq 35 with $j_{l+1}(K) \simeq (1/K) \cos [K - (l + 2)\pi/2]$ for $K \gg 1$, we have

$$b_l(K) = \frac{(l-1)!!}{l!!} b_0(K) + O(K^{-2})$$

We have now an expression for matrix $\mathbf{W}_\infty$ as

$$\mathbf{W}_\infty = b_0(K)^2 \tilde{\mathbf{W}}_\infty \tag{A.2}$$

where $\tilde{\mathbf{W}}_\infty$ is a symmetrical matrix that holds only constant numerical coefficients

$$\tilde{\mathbf{W}}_\infty = [(1/2)\tilde{\mathbf{s}}\tilde{\mathbf{s}}^{\mathrm{T}} - \tilde{\mathbf{P}}\mathbf{Q}\tilde{\mathbf{P}}] \tag{A.3}$$

$$\{\tilde{\mathbf{s}}\}_l = (-1)^{1/2}(2l + 1)^{1/2} \frac{(l-1)!!}{l!!} \tag{A.4}$$

$$\{\tilde{\mathbf{P}}\}_{lp} = \left[\frac{2p + 1}{2l + 1}\right]^{1/2} \sum_{n:\text{even}} (-1)^{n/2}(2n + 1) \frac{(n-1)!!}{n!!} C(pnl;000)^2 \tag{A.5}$$

Since it was difficult to evaluate $\tilde{\mathbf{W}}_\infty$ analytically, we numerically evaluated eq A.3. Results of computation showed that every matrix elements of $\tilde{\mathbf{W}}_\infty$ is less than or equal to $O(1)$ in the order of magnitude.

From eq A.1 and A.2, it is evident that at $\mathbf{k} \rightarrow 0$, matrix $\mathbf{\Phi}$ is diagonal, and at $\mathbf{k} \rightarrow \infty$, matrix $\mathbf{\Phi}$ reduces to an identity matrix, because every matrix element of $\mathbf{W}$ is $O(\{kL\}^{-2})$. From this, we have

$$\lim_{lL \rightarrow 0} A(kL,\nu) \simeq 1 + \pi\nu b L^2/2 \tag{A.6}$$

$$\lim_{kL \rightarrow \infty} A(kL,\nu) \simeq 1 + \pi\nu b L^2/2 \cdot (\pi/kL)^2 O(1) \tag{A.7}$$

Supplementary Material Available: A source program, written in Microsoft FORTRAN V.4.01, that computes $g(\mathbf{k},t)$ at delay times of 0 s and 1 μs to 0.5 s in steps of 1, 2, and 5 and test input data and results of computation (77 pages). Ordering information is given on any current masthead page. See also ref 7.

References and Notes

(1) Doi, M.; Shimada, T.; Okano, K. *J. Chem. Phys.* **1988**, *88*, 4070.

(2) Maeda, T.; Fujime, S. *Macromolecules* **1984**, *17*, 1157.

(3) Rose, M. E. *Elementary Theory of Angular Momentum*; John Wiley & Sons: New York, 1957.

(4) Moriguchi, S.; Udagawa, K.; Hitotsumatsu, S. *Mathematical Formulas* (In Japanese); Iwanami: Tokyo, 1960.

(5) Berne, B. J.; Pecora, R. *Dynamic Light Scattering*; John Wiley & Sons: New York, 1976; section 8.7.

(6) Doi, M.; Edwards, S. F. *The Theory of Polymer Dynamics*; Clarendon Press: Oxford, 1986.

(7) The program, written on a 5.25 in., 1.2 MB diskette in PC-DOS format, is available on request from the author.

(8) DJSPHB and DSICI are subroutines in Nippon Data General's Scientific Subroutine Package.

(9) Smith, B. T.; Boyle, J. M.; Dongarra, J. J.; Garbow, B. S.; Ikebe, Y.; Klema, V. C.; Moler, C. B. Matrix Eigensystem Routines—EISPACK Guide. *Lecture Notes in Computer Science*, 2nd ed.; Springer-Verlag: Berlin, 1976; Vol. 6.

(10) Press, W. H.; Flannery, B. P.; Teukolsky, S. A.; Vetterling, W. T. *Numerical Recipes—The Art of Scientific Computing*; Cambridge University Press: Cambridge, 1986.

(11) Dongarra, J. J.; Moler, C. B.; Bunch, J. R.; Stewart, G. W. *LINPACK Users' Guide*; SIAM: Philadelphia, 1979.

(12) Conte, S. D.; de Boor, C. *Elementary Numerical Analysis—An Algorithmic Approach*, 3rd ed.; McGraw-Hill: Kogakusha: Tokyo, 1980.

(13) Abramowitz, M.; Stegun, I. A. *Handbook of Mathematical Functions—With Formulas, Graphs, and Mathematical Tables*; Dover: New York, 1972.

(14) Yamakawa, H. *Modern Theory of Polymer Solutions*; Harper and Row: New York, 1971.

(15) Zimm, B. H. *J. Chem. Phys.* **1946**, *14*, 164.

(16) Fujita, H.; Teramoto, A.; Yamashita, T.; Okita, K.; Ikeda, S. *Biopolymers* **1966**, *4*, 781.

(17) Itou, S.; Nishioka, N.; Norisuye, T.; Teramoto, A. *Macromolecules* **1981**, *14*, 904.

(18) Doi, M.; Edwards, S. F. *J. Chem. Soc., Faraday Trans. 2* **1978**, *74*, 560.

(19) Teraoka, I.; Mori, Y.; Ookubo, N.; Hayakawa, R. *Phys. Rev. Lett.* **1985**, *55*, 2712.

(20) Doi, M.; Yamamoto, I.; Kano, F. *J. Phys. Soc. Jpn.* **1984**, *53*, 3000.

(21) Russo, P. S.; Karasz, F. E.; Langley, K. H. *J. Chem. Phys.* **1984**, *80*, 5312.

(22) Maeda, T.; Fujime, S. *Macromolecules* **1985**, *18*, 2430; correction to typographical errors is in *Macromolecules* **1986**, *19*, 1494.

(23) Fujime, S.; Takasaki-Ohsita, M.; Maeda, T. *Macromolecules* **1987**, *20*, 1292.

(24) This b value is different from the one given in ref 21. There are three ways to estimate the b value from A_2, $\bar{v}_2$, and M/L: The first is to use the relation $A_2 = \bar{v}_2 L/bM$, the second $A_2 = (\pi/4)bL^2N_{\mathrm{A}}/M^2$, and the third $\bar{v}_2 = (\pi/4)b^2L(N_{\mathrm{A}}/M)$. Using $A_2 = 3.2 \times 10^{-4}$ (cm^3 mol)/g^2, $L = 205.5$ nm, $M = 3.0 \times 10^5$ Da, and $\bar{v}_2 = 0.791$ cm^3/g, we have $b = 1.69$ nm from the first relation, $b = 1.44$ nm from the second one, and $b = 1.56$ nm from the last. Russo et al. gave a diameter value 1.6 nm in their paper, adopting the first b value (with a typographical error). We adopt the second one, because we compute $\mathbf{\Phi}$ using eq 25. In order to obtain the correct A_2 value at $\mathbf{k} = 0$ in our computation, we have to use the second relation in the above to estimate the b value.

(25) Riseman, J.; Kirkwood, J. G. *J. Chem. Phys.* **1950**, *18*, 512.

(26) Broersma, S. *J. Chem. Phys.* **1960**, *32*, 1626, 1632.

(27) Newman, J.; Swinney, H. L. *J. Mol. Biol.* **1977**, *116*, 593.

(28) Berkowitz, S. A.; Day, L. A. *J. Mol. Biol.* **1976**, *102*, 531.

(29) The A_2 value given here was recalculated using the corrected M value.[27]

(30) Maeda, T.; Fujime, S. Unpublished results. See also Figures 4 and 7 of ref 22.

(31) Pusey, P. N. *J. Phys. A* **1978**, *11*, 119.

(32) Tanford, C. *Physical Chemistry of Macromolecules*; John Wiley & Sons: New York, 1961.

(33) Kubota, K.; Chu, B. *Biopolymers* **1983**, *22*, 1461.